Experiment 7

Electron Spin Resonance

7.1 Introduction: The Landé g Factor

Electron Spin Resonance (ESR) is, in many regards, strikingly similar to nuclear magnetic resonance. The fundamental premise is that by applying a static uniform magnetic field to a population of electronic spins, one will break the 2-fold spin degeneracy of the spin $\frac{1}{2}$ particles via the Zeeman effect. The energy gap between the spin down and spin up states is given by

$$\Delta U = \hbar\omega_o = \gamma\hbar B_0 \tag{7.1}$$

where $\hbar\omega_o$ is the photon energy corresponding to the energy splitting ΔU, B_0 is the magnitude of the applied magnetic DC field and γ is the appropriate magnetogyric ratio for the electron. For an electron, one frequently sees γ expressed as

$$\gamma = g\mu_B \tag{7.2}$$

where g is the Landé factor and μ_B is the Bohr magneton. The Landé factor effectively sets the ratio between the magnetic moment and the total spin of the electron and there are many subtleties hidden within this constant. For a free electron, $g = 2.0023$. However, as you will discover within this experiment, one rarely observes this value because experiments are typically performed on electrons inside materials, not electrons isolated in vacuum. Rather, the value of g becomes *renormalized* by interactions between the electron and its surroundings.

The thermal occupation factors for the two spin states will be governed by Boltzmann statistics, and at any sufficiently low temperature T such that $\Delta U/kT \gg 1$ there will be an excess of spins in the lower energy state, hence a net magnetization. As with NMR, one can manipulate this net magnetization in order to perform measurements on the electron spins. In particular, by supplying a radiofrequency (rf) wave at the resonant photon energy $\hbar\omega_o$ that is polarized perpendicular to the DC magnetic field, one can move spins into the higher energy state. This is the phenomenon of ESR, and measurements of the conditions for resonance can be used to infer properties of the electronic spins.

This very brief introduction into the theory of ESR is meant to simply whet the appetite. For a more thorough discussion of the elements of magnetic resonance, I strongly recommend that the student read sections 5.1 and 5.2 of Experiment 5, Pulsed Nuclear Magnetic Resonance. In particular, the discussion that will follow assumes familiarity with the two-level system and relaxation dynamics.

7.2 Experimental Approach

Given Eq. 7.1, one can see that there are two possible ways to search for ESR for any given sample: one can either adjust B_0 with the photon energy $\hbar\omega_o$ fixed or one can adjust $\hbar\omega_o$ with B_0 fixed. In either case, one scans one variable and then monitors an output signal from the sample in search of resonance. In a modern day NMR experiment, one typically fixes the applied magnetic field and then one scans in frequency until resonance is observed; this is certainly quite feasible given modern rf and microwave synthesizers. However, ESR is a field with a far longer history and in the days before solid state electronics it was often easier to build a stable rf source that operated at a single fixed frequency and then one swept the magnetic field. It is this latter approach which has been taken in the design of the ESR experiment in our laboratory.

Of course, it is impractical to consider continuously adjusting B_0 generated by a large DC electromagnet over any reasonably short timescale. For this reason, the ESR apparatus contains a second electromagnet that operates at a very low modulation frequency (60 Hz) that is aligned coaxially with the DC electromagnet.

Provided that the modulation frequency is much smaller than the fixed rf (340 MHz in our apparatus), then the resulting external magnetic field can be considered as a time varying DC magnetic field:

$$B_0(t) = B_0^{DC} + B_0^{mod} \sin(\Omega_{mod} t) \tag{7.3}$$

This allows one to scan over a DC magnetic field range of $B_0^{DC} \pm B_0^{mod}$ without having to adjust the large DC electromagnet.

The populations of electronic spins to be studied are in the form of solid samples inside glass vials. The sample is placed inside an rf coil situated at the centre of the electromagnet with its axis aligned perpendicular to the direction of the DC magnetic field, as sketched in Fig. 7.2:

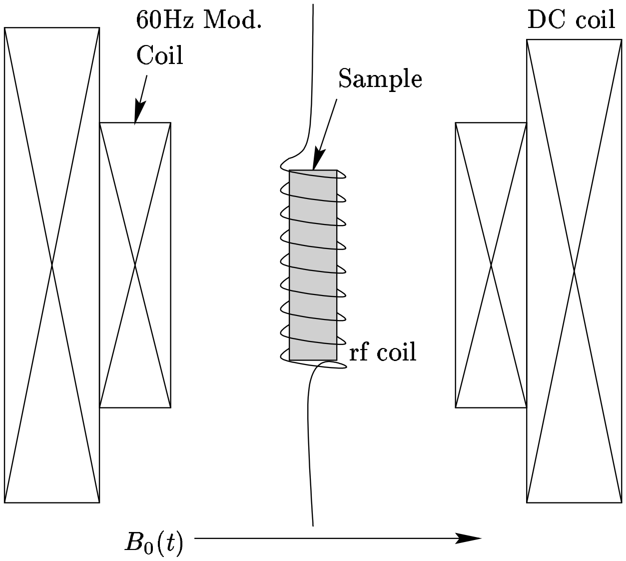

Figure 7.1: A sketch of the core of the ESR apparatus. The sample to be studied is placed inside an rf coil at the centre of the electromagnet, such that the axis of the coil is perpendicular to the applied DC magnetic field.

The rf coil is continuously driven at 340 MHz, thereby immersing the sample in a relatively uniform rf magnetic field that is perpendicular to the DC magnetic field. When $B_0(t)$ does not satisfy the resonance condition for the sample, then the sample is effectively invisible and the rf coil behaves like an empty solenoid. The rf voltage induced across the coil will be

$$v(t) = i(t)\ \imath\omega_o L \tag{7.4}$$

where $i(t)$ is the rf current driving the coil and L is the usual expression for the inductance of a solenoid with N turns and cross sectional area A:

$$L = \mu_o N^2 A \tag{7.5}$$

When the conditions for resonance are satisfied, then the interior of the coil becomes paramagnetic and one must replace μ_o in Eq. 7.5 by the more general expression $\mu = \mu_o(1+\chi)$ where χ is the magnetic susceptibility of the sample. At nonzero frequency, χ will have both a real (in phase) and imaginary (quadrature) component, $\chi = \chi' - \imath\chi''$, and the voltage across the solenoid will become

$$v(t) = i(t)\ \left(\omega_o \mu_o \chi'' N^2 A + \imath\omega_o \mu_o (1+\chi') N^2 A\right) \tag{7.6}$$

Note that this voltage has both a resistive (in phase) and inductive (quadrature) component. χ' effectively modifies the inductance of the coil while χ'' introduces losses into the coil - this signal comes from power absorption by the electron spins in the sample. To detect the absorption signal, a so called marginal oscillator

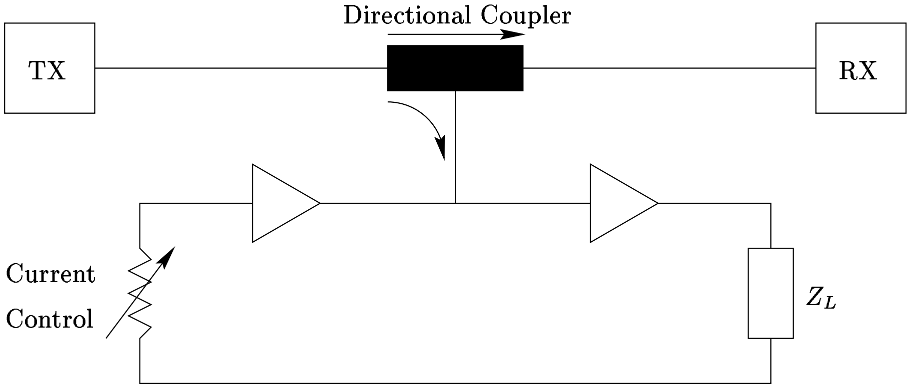

Figure 7.2: Schematic drawing of a marginal oscillator circuit. Radiofrequency power is emitted from the transmitter TX. The amplifiers drive the closed loop into saturation, regardless of the variation of the impedance of the load Z_L. Losses in Z_L translate into reduced power reaching the receiver RX.

circuit is employed. The idea is to supply a fixed amount of rf power to the resonant element (the rf coil) by using a closed loop feedback system, as depicted in Fig. 7.2.

Here TX represents the rf source, RX the rf receiver and Z_L the impedance load (the rf coil). A directional coupler leaks a small amount of rf power out of a transmission line into the closed loop feedback circuit. Two high gain amplifiers drive the closed loop into saturation at a specified current that is controlled by a rheostat (the current control knob on our apparatus). As B_0 is swept through the resonance condition of the sample, Z_L momentarily develops a real resistance and the current in the circuit starts to drop. In response to the dropping current, more power is removed from the transmission line in order to maintain saturation. The result is that rf power received at RX drops when Z_L absorbs power. A plot of output at RX vs B_0 then indicates the field strength at which ESR occurs.

A Tektronix digital oscilloscope will be made available for data collection. By connecting a sample of the 60 Hz modulation signal to Channel 1 and the rf receiver output to Channel 2 once can generate plots similar to those sketched in Fig. 7.3. To obtain plots in the form of Fig. 7.4 one merely needs to change the oscilloscope display mode to XY mode in which Channel 1 becomes the X axis and Channel 2 becomes the Y axis.

7.3 Calibration Using DPPH as a Standard

Unfortunately time has been less than kind to the ESR apparatus and so there are a few practical problems that need to be resolved prior to performing an experiment. First and foremost, one must calibrate $B_0(t)$. A second critical problem is that there is a phase lag between the 60 Hz modulation signal and the ESR signal that needs to be corrected.

The large DC electromagnet is driven by a 10 Ampere current source and the current I_{DC} can be accurately monitored by a digital multimeter. The electromagnet is formed from bands of high conductivity copper wrapped around soft iron pole pieces. As current flows through the copper it eventually dissipates energy as heat which then warms the copper and changes its resistance; therefore, the value of B_0^{DC} will drift with time. For this reason, one should turn on the cold water line for at least 20 minutes prior to conducting an experiment. Another problem with the DC electromagnet is that it has developed a permanent magnetization, $B_0^{permanent}$. Finally, the 60 Hz modulation coils are uncalibrated, but one can monitor the voltage supplied to them v_{mod} with the oscilloscope. Gathering all of this information together, one can now write an expression of $B_0(t)$ as a function of I_{DC} and v_{mod}.

$$B_0(t) = B_0^{permanent} + \alpha I_{DC} + \beta v_{mod} \sin(\Omega_{mod} t) \tag{7.7}$$

One now needs to devise a means of determining the three unknowns $B_0^{permanent}$, α and β. For this

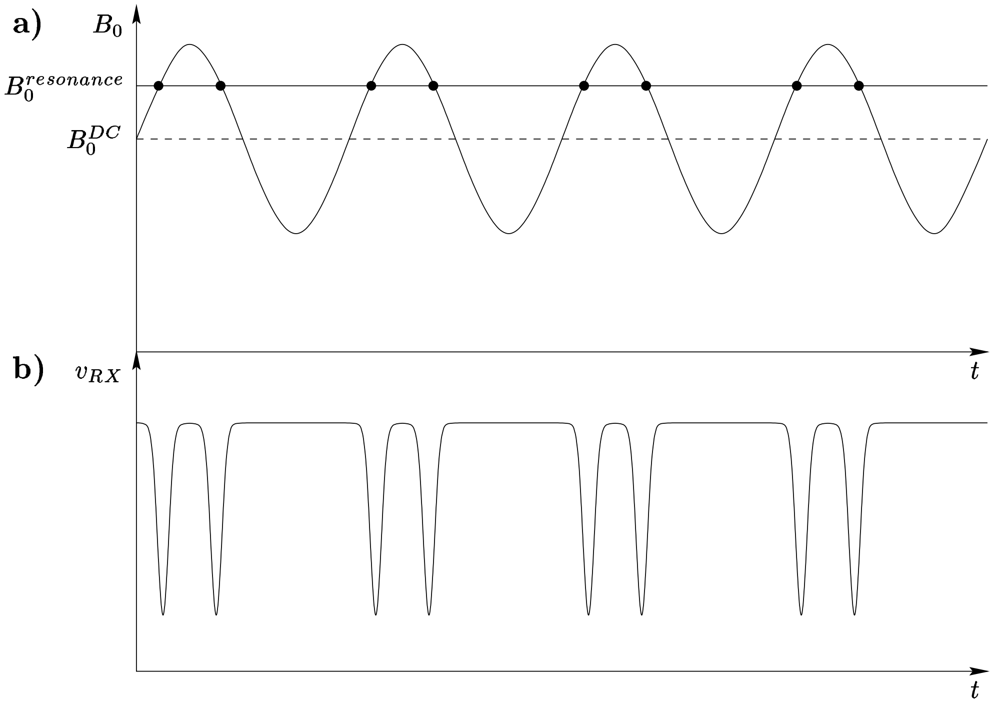

Figure 7.3: a) Variation of the DC field $B_0(t) = B_0^{DC} + B_0^{mod}\sin(\Omega_{mod}t)$. When $B_0(t) = B_0^{resonance}$, the field at which Eq. 7.1 is satisfied for the supplied rf, then ESR occurs. b) The voltage output of the rf receiver drops when ESR occurs.

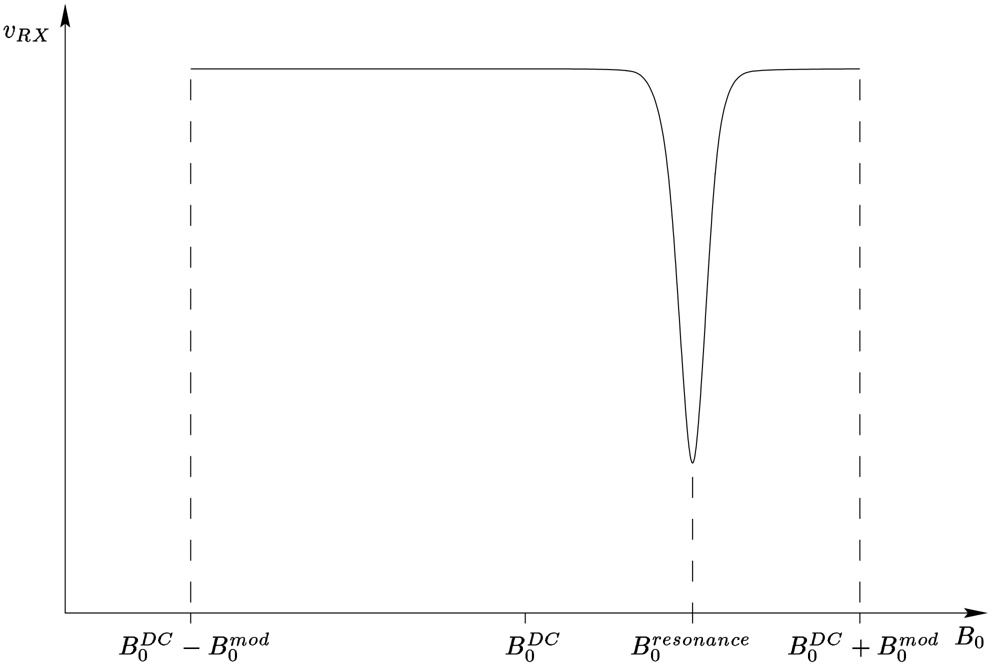

Figure 7.4: The data plotted as v_{RX} vs B_0. The data from the field sweep spans $B_0^{DC} \pm B_0^{mod}$ with the resonance visible at $B_0^{resonance}$.

reason, one employs a calibration standard whose ESR we can accurately predict. Diphenyl-picrly-hydrazyl (DPPH) is an organic salt that has one approximately free electron that behaves like a spin $\frac{1}{2}$ system with $g = 2.0036$ and a very narrow resonant lineshape. Given this value for g, one can calculate the resonant field strength B_0^{DPPH} from Eqns. 7.1 and 7.2 and then use it in Eq. 7.7 to devise a calibration scheme.

As mentioned earlier, a second key problem is that there is a phase lag between v_{mod} and v_{RX} that has been introduced somewhere within the electronics. Therefore, the pictures shown in Fig. 7.3 appear slightly out of phase and one could draw the erroneous conclusion that ESR occurs at two different values of B_0. To rectify this matter, a simple phase shifting circuit should be constructed and inserted between the 60 Hz source and the oscilloscope. The circuit can be adjusted manually and the signal inversion option on the oscilloscope activated to put the modulation signal and the rf output signal back into phase.

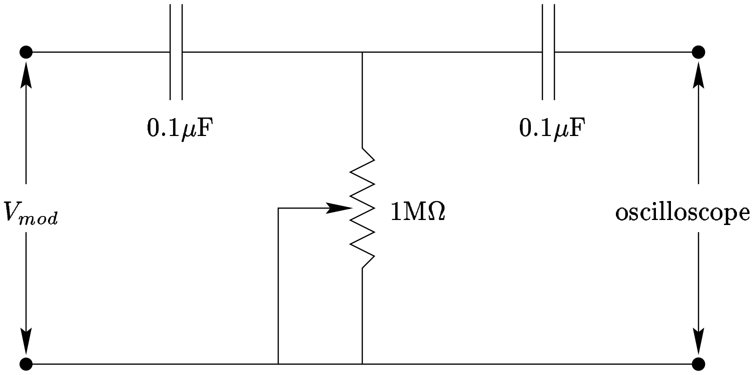

Figure 7.5: A simple phase shifting circuit used to correct for a phase lag in the ESR electronics.

To complete the calibration procedure, one must solve for the three unknowns in Eq. 7.7, however one has only two experimental parameters to adjust: I_{DC} and v_{mod}. Therefore, one must invoke an independent means of determining one of the unknowns. A digital Hall probe will be made available for measurement of the DC magnetic field, however be aware that it may have its own calibration problems as well. Nonetheless, this allows one to measure $B_0^{DC} = B_0^{permanent} + \alpha I_{DC}$ in a very direct manner. *It is recommended that the student measure* B_0^{DC} *as a function of* I_{DC} *over the range* $0 \to 1$ *A for both increasing and decreasing current. Are there any signs of hysteresis?* **Adjust the DC current very slowly to avoid courting severe hysteresis.** *Finally, use the resonance condition for DPPH to calibrate the AC field strength parameter,* β*. If* $B_0^{permanent}$ *is very small and hysteresis is not present, then the DPPH resonance can be used to give both* α *and* β *independent of the Hall probe.*

7.4 Measurement of g in $Cu(SO_4) \cdot 5H_2O$

Recall that the Landé g factor for a free electron is 2.0023 while that of one of the electrons in DPPH is 2.0036 . Why do these values differ? To see how a 'free electron' picture of ESR can break down in solids, consider the crystalline material copper sulfate pentahydrate, $Cu(SO_4) \cdot 5H_2O$. The copper in this solid is ionically bonded as Cu^{2+} to the sulfate radical ${SO_4}^{2-}$, and therefore has one unpaired electron in its $3d$ orbital. Now one must account for not only the $s = \frac{1}{2}$ *spin angular momentum*, but also the $\ell = 2$ *orbital angular momentum* as well. Quantum mechanics predicts that there will be $(2\ell + 1)(2s + 1) = 10$ degenerate ground states if there is no spin-orbit coupling and no external fields acting on the Cu^{2+} ion.

Fortunately, nature is kind to us in that the unpaired electron does indeed behave almost like a free spin $\frac{1}{2}$ particle due to the very complexity of the problem. First, the spin and orbital angular momentum do indeed couple into a net angular momentum $\vec{J} = \vec{L} + \vec{S}$. Second, the Cu^{2+} ions reside inside a crystal lattice, not in vacuum, so each ion experiences a net electric field generated by its surroundings (nearby atoms). Let this net electric field at the ion of interest be called a *crystal field.* Since each orbital angular momentum index ℓ corresponds to a different electronic wavefunction (with a different spatial distribution with respect to the crystal lattice), then one anticipates that the crystal field will lift the $2\ell + 1 = 5$-fold orbital degeneracy. This is indeed the case for $Cu(SO_4) \cdot 5H_2O$ and the details of how the crystal field lifts the degeneracy depend very sensitively upon the symmetry of the crystal lattice.

Though the topic of *effective Hamiltonians* which obey discrete symmetries is beyond the scope of this course, I ask that the student appreciate that what seems like an impossible problem to solve can, in fact, be solved via an appropriate ansatz; instead of attempting to write an exact expression for the crystal field at the ion, one simply builds up a Hamiltonian that will reflect the symmetry of the crystal lattice, which will have the same symmetry as the crystal field.

$$H_{eff} = \sum_{p,q} B_p^q O_p^q \tag{7.8}$$

Here, B_p^q are numerical prefactors and O_p^q are the so called *Stevens operators*, which are merely the spherical harmonics Y_p^q with the substitution of angular momentum operators for position: $(x, y, z) \rightarrow (J_x, J_y, J_z)$. Crystal symmetry and the total angular momentum dictates which values of p are allowed (the spherical harmonics must have the same or less symmetry than the crystal and the value of $j = \ell + s$ sets the maximum number of angular momentum operators). Only even values of q are allowed due to time reversal symmetry (the crystal field is viewed as a field that has always existed and always will, hence the direction of time is irrelevant; odd values of q introduce odd numbers of $\vec{J}$ operators which do not obey time reversal symmetry). Therefore, there is a finite set of O_p^q which are allowed in the effective Hamiltonian, and the only unfinished task is determining the prefactors B_p^q. These are frequently chosen to fit experimental observations made with a high field ESR apparatus. Through feedback between experiment and theory, an effective Hamiltonian of the form Eq. 7.8 can be constructed for a given crystal.

A schematic picture of the energy splitting in the tetragonal crystal $Cu(SO_4) \cdot 5H_2O$ is shown in Fig. 7.6. Most notable is the fact that the tetragonal symmetry does lift the 5-fold orbital degeneracy, but in doing so the resultant electronic states have become a nontrivial admixture of the eigenstates of $\vec{L}$ and $\vec{S}$, and so one cannot label the states using the allowed values of $m_\ell = -2, -1, 0, 1, 2$. Rather, I have chosen the arbitrary labels E_1, E_2, E_3, E_4, E_5.

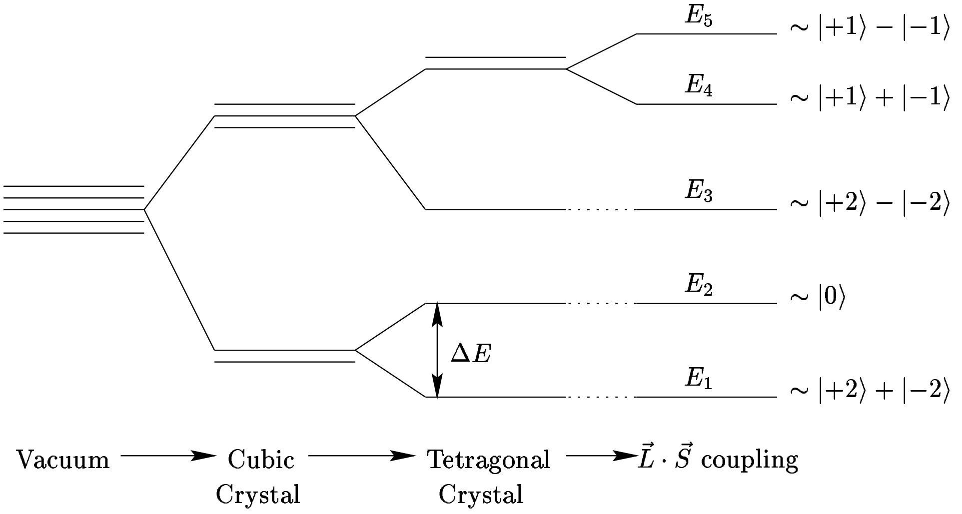

Figure 7.6: The splitting of the 5-fold orbital degeneracy of an $\ell = 2$ electron in a tetragonal crystal.

Given the energy spectrum shown in Fig. 7.6, one can see that there could very well be many allowed transitions and therefore ESR on $Cu(SO_4) \cdot 5H_2O$ could be quite complicated. Fortunately, there is one more simplification: temperature. It is known from calculations and experiment that the spacing between the electronic energy levels of Cu^{2+} in $Cu(SO_4) \cdot 5H_2O$ is on the order of $\Delta E \sim 10^4$ cm^{-1} (2×10^{-19} J) while the thermal energy at room temperature is roughly $kT \sim 4 \times 10^{-21}$ J. Therefore, one is working in a regime where $\Delta E/kT \gg 1$, which means that it is reasonable to assume that only the lowest energy state, E_1, is occupied. Recall that the thermal occupation factor for a given state is governed by Boltzmann statistics:

$$N_i = \frac{e^{-E_i/kT}}{Z} = \frac{e^{-E_i/kT}}{\sum_{j=1}^{5} e^{-E_j/kT}} \tag{7.9}$$

where Z is the partition function. We can arbitrarily set $E_1 = 0$ and measure all energies with respect to this reference point with $E_2 \sim \Delta E$, $E_3 \sim 2\Delta E$ and so forth. One can then see that if $\Delta E/kT \gg 1$, then $N_1 \sim 1$, $N_2 \sim e^{-50}$, $N_3 \sim e^{-100}$ .... Therefore, one can approximate the behaviour of the system by concentrating solely upon the energy level E_1. Now consider subjecting the system to an external DC magnetic field. This will lift the 2-fold spin degeneracy of each state, but only E_1 will contribute to any observed ESR lineshape. The end result is that the seemingly complicated energy spectrum of the Cu^{2+} ion in $Cu(SO_4) \cdot 5H_2O$ in an external magnetic field can be reduced to the archetypal 2-level system as discussed in the introduction to Experiment 5, Pulsed Nuclear Magnetic Resonance.

How does this situation differ from that of ESR on a free electron? Referring to Fig. 7.6, one can see that the lowest energy state E_1 is a coherent mixture of the $m_\ell = -2$ and $+2$ states. Therefore, when this state is split by the application of B_0^{DC}, the resulting states have total angular momentum that differs from the usual $\pm\frac{1}{2}$. However, it is still convenient to treat the system as having spin $\frac{1}{2}$ and so by Eq.7.2 if I don't modify the magnetic moment μ_B, then I must modify the Landé g factor. To conclude, the complexities of the $3d^9$ orbital of Cu^{2+} result in an enhancement of g. This then forms the primary objective of the ESR experiment: using the position of the ESR absorption, calculate g for the unpaired electron of Cu^{2+} in $Cu(SO_4) \cdot 5H_2O$. A polycrystalline sample is available for which one can obtain a mean value of g for this particular compound.

7.5 Selected References

C.P. Slichter, Principles of Magnetic Resonance. Springer-Verlag, New York U.S.A., 1978.

This text should be considered essential reading for those who wish to truly understand NMR. If a copy cannot be found in the library, then contact the teaching assistant.

D.J. Griffiths, Introduction to Quantum Mechanics. Prentice-Hall, Englewood Cliffs, U.S.A., 1994

I think this is the QM textbook used in your 4th year class. However, every elementary QM textbook should cover Larmor precession of an electron in a magnetic field.